Original Russian Text © N.S. Rukk, R.M. Zakalyukin, A.Yu. Skryabina, 2016, published in Tonkie Khimicheskie Tekhnologii, 2016, Vol. 11, No 1, pp. 5-22.

CHEMISTRY AND TECHNOLOGY OF INORGANIC MATERIALS

LANTHANIDE OXYIODIDES

N.S. Rukk[@], R.M. Zakalyukin, A.Yu. Skryabina

Moscow Technological University (Institute of Fine Chemical Technologies), Moscow, 119571 Russia
[@] Corresponding author e-mail: roukkn@inbox.ru

The present review is devoted to consideration and generalization of a number of synthetic methods for lanthanide oxoiodides preparation as well as to consideration of their structural particularities and thermal stability. Phase diagrams with the participation of REE oxoiodides, alkaline metal iodides or silver iodide are given and discussed. All the systems are characterized by the solid solution formation on the basis of the pure compounds, while the systems with the participation of alkaline metal iodides are characterized by the formation of incongruent melting compounds. Structural data concerning oxoiodides of lanthanides with different oxidation states and with the participation of some other elements (carbon, nitrogen, barium, osmium, etc) are present and overviewed. Possible areas of application (catalysis, X-ray detectors, medical diagnostics) including distinct luminescent properties of Ce-, Pr-, Nd-, Sm-doped REE oxoiodides are underlined.

Keywords: *rare earth elements (REE), iodide, oxoiodides, phase equilibria, crystal structure.*

Introduction

Compounds of lanthanides, first of all, their halides and oxohalides, in particular, iodides are very promising for the production of metal halide lamps, more effective than filament lamps and having no alternative at the power exceeding 5 kW. Metal halide lamps have high values of light output (up to 100 lm/W) and color rendering index (~ 95), and their operating life is about 20000 h [1–3]. Ln^{3+}-doped (Ln = Ce, Pr, Nd, Sm, Eu) oxohalides of rare earth elements (REE) are characterized by promising scintillation properties. Unlike the corresponding halides, they are less hygroscopic and more stable [4–8]. For the practical application of lanthanide oxoiodide crystals as fast scintillators, allowed 5d-4f transitions are important, since the observed luminescence is due to these transitions [6–8]. Scintillators can be used as X-ray emission detectors; for positron emission tomography (PET); and for single-photon emission computed tomography (SPECT). Scintillation crystals activated by REE ions are applied in gamma- and gamma-ray logging detectors for geological exploration and medicine [5, 7].

It is known also [9, 10] that lanthanide iodides, in particular, samarium(II) iodide used in most cases as a tetrahydrofuran (THF) solution in the form of $[Sm(THF)_2I_2]$, are strong Lewis acids and active catalysts in synthetic organic chemistry. It is possible to assume that other iodine- and oxygen-containing REE as well can find application for obtaining compounds having different composition and a required set of properties.

In view of the aforesaid the determination of optimal conditions of synthesis, structural features, phase composition and stability of oxoiodides and related compounds is of great importance.

The literature provides a good deal of data concerning lanthanide halides, although REE iodides still remain least studied [11–43]. The corresponding oxohalides have been known for less than one hundred years: their active studying started only in the 60–70th years of the last century, REE oxochlorides and oxobromides being best studied now.

The purpose of the this review is to systematize and generalize the segmental data on the preparation conditions, structure, thermal stability and some properties of oxoiodides of lanthanides and other related compounds.

METHODS OF PREPARING LANTHANIDE IODIDES OF COMPOSITION LnOI

I. Preparation of lanthanide oxoiodides by the interaction of a metal, its oxide and crystalline iodine according to the following overall reaction [14–16]:

$$Ln + Ln_2O_3 + 1.5\,I_2 = 3\,LnOI\,(Ln = Gd, Dy, Tm, Lu) \qquad (1)$$

In order to decrease the reaction temperature and to increase the product yield finely divided powdered metals are previously obtained by hydrogenation followed by dehydrogenation of ingots of the corresponding lanthanide. The hydrogenation is carried out in a flow of hydrogen at 600–650 °C for 5 h. The resulting brittle hydrides are ground in a mortar and subjected to dehydrogenation in vacuum at 700–750 °C for 3 h

[14–16]. Then mixtures of stoichiometrical amounts of the finely divided metal, iodine and the corresponding oxide are prepared in an inert gas atmosphere. The synthesis is carried out in previously evacuated and soldered quartz ampoules. The formation of the lanthanide oxoiodide proceeds at 500–550°C as a result of two consecutive processes:

$$2\ Ln + 3\ I_2 = 2\ LnI_3 \quad (2)$$

$$LnI_3 + Ln_2O_3 = 3\ LnOI \quad (3)$$

It was shown [14, 15] that iodine starts interacting with the finely divided metallic lanthanide powder at 155–160°C, and at 180–190°C vigorous burning of the metal in iodine occurs to form the iodide and oxoiodide of the lanthanide. The reaction becomes a little slower at 250°C and practically stops at 300°C. However, in the temperatures range of 350–420°C the interaction of the previously formed lanthanide iodide with its oxide occurs again giving the final product, oxoiodide. On the basis of thermal studies a technique of synthesizing lanthanide oxoiodides was developed. According to this technique the synthesis is carried out for 3 h at 500–550°C [14, 15].

The preparation of oxoiodides of REE's activated by other lanthanides (praseodymium, neodymium, samarium and europium) is carried out similarly to the synthesis of non-activated samples from previously obtained activated oxides, finely divided metal powders and elementary iodine [5]. The synthesis is carried out in evacuated and soldered quartz ampoules at 500–550°C for 3 h:

$$Ln + Ln(Ln')_2O_3 + 1.5\ I_2 = 3\ Ln(Ln')OI\ (Ln = Gd,\ Lu;\ Ln' = Pr, Nd, Sm, Eu) \quad (4)$$

All the preliminary operations are performed in a "dry" box in an inert atmosphere.

A variety of this method is the shock synthesis of oxoiodides. The reaction of a stoichiometrical mixture of an oxide, powdered metal and iodine is initiated by double blasting [17, 18]. The composition of the obtained oxoiodide LnOI (Ln = La–Nd, Sm, Gd, Tb, Ho, Lu) precisely corresponds to stoichiometrical. However, the low yield of the product and technological complexity of shock synthesis do not allow this method to become wide-spread in laboratory practice.

II. Interaction of lanthanide oxides with ammonium iodide [17, 19–22]. The interaction of lanthanide oxides with ammonium iodide starts at 260–265ºC and proceeds in two steps. At the first one, a complex of composition $LnI_3 \cdot 3NH_3$ forms:

$$Ln_2O_3 + 6\ NH_4I = 2\ LnI_3 \cdot 3NH_3 + 3\ H_2O, \quad (5)$$

This complex further reacts with unreacted oxide Ln_2O_3 giving the oxoiodide. This is the second step of the process:

$$LnI_3 \cdot 3NH_3 + Ln_2O_3 = 3\ LnOI + 3\ NH_3 \quad (6)$$

The optimal conditions for the synthesis of LnOI (Ln = Gd) were found: Ln_2O_3:NH_4I ratio is 1 : 4, annealing temperature is 370°C, the time of keeping the sample in the furnace is 2 hours [22]. A lower temperature and a larger content of ammonium iodide increase annealing time. It was shown [19, 22] that the temperature of the beginning of lanthanide oxoiodides formation increases in the series La–Gd–Ho and is 300, 330 and 345°C, respectively, whereas the temperature of their decomposition in the same series decreases from 440 (Ln = La) to 400 (Ln = Gd) and 390 (Ln = Ho). It was noted [21] that the interaction of yttrium oxide and ammonium iodide proceeds vigorously and in one step, the formed yttrium oxoiodide being decomposed practically at once.

A synthesis of lanthanum oxoiodide by the interaction of La_2O_3 and NH_4I taken in a molar ratio of 1:2 upon heating is described [17, 19]. Lanthanum oxoiodide is obtained also when heating La_2O_3 + LaI_3 mixture at 750°C for 10 h [23]. The reactions should be carried out in the dark, in evacuated quartz ampoules, and all manipulations with the starting substances and reaction products – in an inert atmosphere (argon).

III. Oxidation of lanthanide iodides with oxygen [17, 24].

Single-phase praseodymium oxoiodide is obtained according to the following reaction:

$$PrI_{3(liq)} + ½\ O_2 = PrOI_{(solid)} + I_{2(gas)} \quad (7)$$

Praseodymium iodide is melted in a graphite container (to prevent the interaction of PrI_3 with quartz). Then oxygen is passed at its partial pressure about 0.133 Pa [24]. A method for synthesizing scandium oxoiodide with the use of oxygen impurity at sublimation of previously obtained scandium(III) iodide [25], as well as in the course of obtaining LaOI [26] are described.

IV. Interaction of lanthanide iodides with antimony(III) oxide [26–28]:

$$3LnI_3 + Sb_2O_3 = 3LnOI + 2SbI_3 \quad (8)$$

A stoichiometrical mixture of anhydrous lanthanide iodide and antimony oxide prepared in a box in the absence of

moisture and oxygen is placed in a quartz reactor. The latter is evacuated to attain a pressure of about 1 Pa and soldered. The reactor is heated slowly in a tube furnace to 400°C and maintained at this temperature within several hours to remove volatile antimony triiodide that is condensed in the cold part of the quartz tube. In some cases in order to improve the crystallinity of the samples the formed oxoiodide is heated to 700°C without its further decomposition.

V. Thermal decomposition of crystalline hydrates of lanthanide iodides [29].

The decomposition process can be presented as follows:

$$YI_3 \cdot 6H_2O\ (160°C) = YI_3 \cdot 5H_2O\ (210°C) = YI_3 \cdot 3H_2O\ (240°C) = Y(OH)_2I \quad (9)$$

The final product is a mixture of composition YOI + Y_2O_3 [29]. Samarium, thulium and ytterbium oxoiodides can be obtained similarly by heating crystalline hydrates of their iodides in a flow of air [28]. Dehydration of europium(III) iodide hexahydrate in high vacuum gives at first europium(II) iodide. The latter is kept in a flow of humid air at 100°C until iodine evolution ceases. The resulting product is heated in vacuum or kept at 750°C for 8 h in nitrogen atmosphere. In the latter case microcrystals of europium oxoiodide are obtained [28]. Dysprosium oxoiodide is obtained similarly, by calcination of dysprosium iodide a flow of air flow followed by keeping at 200°C in vacuum.

VI. Evaporation of an aqueous solution of lanthanide iodide.

In some cases an aqueous solution saturated with ammonium iodide is used. The aqueous solutions are evaporated to dryness, and the solid residue is heated to 550°C in order to remove volatile by-products. Samarium, thulium and ytterbium oxoiodides can be obtained by this method [17, 30].

VII. Solid-phase synthesis by lanthanide oxide interaction with its iodide according to the following reaction [4, 28]:

$$Ln_2O_{3(solid)} + LnI_{3(solid)} = 3\,LnOI_{(solid)} \rightarrow (Ln = Y, La, Gd, Lu) \quad (10)$$

A mixture of an iodide and oxide of the corresponding lanthanide obtained in a "dry" box in argon atmosphere is kept in a closed quartz ampoule at 1000°C for 10 h. Erbium oxoiodide is obtained similarly in a tantalum floating trough at 1050°C [30].

The main methods for the preparation of lanthanide oxoiodides are shown in fig. 1.

PREPARATION OF LANTHANIDE OXOIODIDES WITH LOW OR VARIOUS OXIDATION DEGREES

In order to obtain these compounds it is necessary to enter a reducer into the system: for example, metallic sodium or barium, organic compounds (for example, thiocarbamide), etc. Reactions proceed better in the presence of a catalyst, for example, lithium cyanamide [31–34].

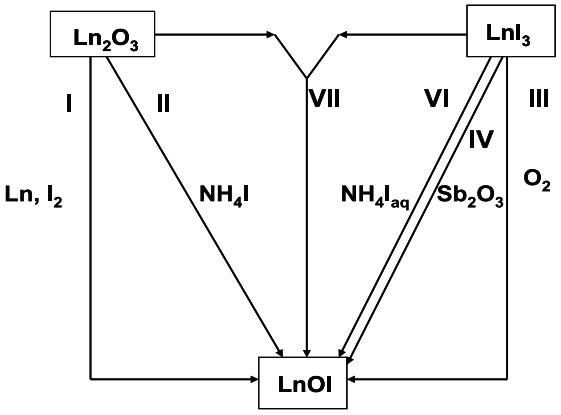

Fig. 1. Scheme for preparation of lanthanide oxoiodides: **I** – interaction of a metal, its oxide and crystalline iodine; **II** – interaction of lanthanide oxides with ammonium iodide; **III** – oxidation of lanthanide iodides with oxygen; **IV** – interaction of lanthanide iodides with antimony(III) oxide; **VI** – evaporation of ammonium iodide-saturated aqueous solution of lanthanide iodide; **VII** – solid-phase synthesis by lanthanide oxide interaction with its iodide[1].

Paper [31] describes a method of obtaining tetrasamarium hexaiodide oxide of Sm_4OI_6 ($SmO \cdot 3SmI_2$) by the interaction of samarium(III) iodide, samarium(III) oxoiodide (previously obtained from SmI3 and Sm_2O_3), sodium iodide and metallic sodium taken in a molar ratio of 3:1:1:4. A tantalum tube is filled with the mixture. The latter is pressurized and placed in a quartz ampoule, which is evacuated and soldered. The synthesis is carried out at 630°C for 96 h. The mixture is cooled to 500°C at a rate of 1°C/h, and then allowed to cool down to room temperature with the furnace off. The proceeding reactions can be written as follows:

$$SmI_3 + Na = SmI_2 + NaI \quad (11)$$

$$SmOI + Na = SmO + NaI \quad (12)$$

$$SmO + 3SmI_2 = Sm_4OI_6 \quad (13)$$

As a result black column-shaped Sm_4OI_6 crystals are obtained.

A synthesis of disamarium iodide dioxide Sm_2O_2I

[1]Method V (thermal decomposition of lanthanide iodide crystal hydrates) is not shown in Fig. 1.

(SmOI·SmO) is described in [33]. First, samarium(II) iodide is obtained by the interaction of metal samarium with iodine under slow heating to 800°C in quartz ampoules. It contains slight impurities of oxygen, which, as shown above, is sufficient for the formation of disamarium iodide dioxide. Samarium(II) iodide is mixed with the stoichiometrical amount of sodium (1:1) and placed into tantalum containers pressurized by welding in argon atmosphere, and then – into quartz ampoules in order to prevent tantalum oxidation. The sample is maintained at 650°C for 168 h and slowly cooled in the air to room temperature. Dark-red needle-shaped Sm_2O_2I crystals with metallic luster are obtained as a mixture with SmI_2, NaI and Sm.

Tetraeuropium hexaiodide oxide Eu_4OI_6 ($EuO·3EuI_2$) [32] is synthesized by europium(II) iodide interaction with lithium cyanamide $Li_2(NCN)$. A mixture of stoichiometrical quantities (1:1) is prepared in a box in the atmosphere of dry argon, placed in tantalic ampoules pressurized in argon atmosphere, and then soldered in quartz ampoules. The sample is kept at 800°C for 48 h and cooled to room temperature at a rate of 6°C/min.

Europium diiodide-oxide Eu_2OI_2 (EuOI·EuO) [35] is synthesized from a 1:1 mixture of europium(II) iodide and Eu_4OI_6. The reagents are previously obtained from metal europium and iodine with the subsequent addition of metallic barium and ammonium iodide. All operations are performed in a "dry" box in an inert gas atmosphere. Tantalum ampoules are filled with the mixture and pressurized in an inert atmosphere with subsequent evacuation and soldering in quartz ampoules. The reaction mixture is kept at 780°C for 10 h and cooled to 500°C at a rate of of 1°C/h, and then – to room temperature with the heating off. A method was suggested for obtaining Eu_2OI_2 by the addition of thiocarbamide to initial europium(III) iodide nonahydrate previously obtained from europium carbonate and hydroiodic acid [europium iodide:thiocarbamide mass ratio is (5.10÷5.30):1]. Then the mixture is heated at a rate of 8–12 °C/min up to 270–32°C, kept for 1–2 h and cooled to room temperature at a rate of 3–5°C/min, which allows obtaining Eu_2OI_2 in a high yield [34].

When attempting to synthesize $BaLnI_4$ by the metallothermic reduction of Ln(III) iodides (Ln = La, Ce) with metallic barium due to oxygen (or nitrogen) microimpurities in the starting substances, $La_9O_4I_{16}$ = $\mathbf{La_3^{II}La6^{III}O_4I_{16}}$, $Ce_9Z_4I_{16}$ and $BaLa_4Z_2I_8$ were isolated [36, 37]:

$$2\ LaI_3 + Ba = 2\ LaI_2 + BaI_2 \quad (14)$$

$$BaI_2 + LaI_2 = BaLaI_4 \quad (15)$$

$$9\ BaLaI_4 + 2\ O_2 = La_3^{II}La_6^{III}O_4I_{16} + 9\ BaI_2 + I_2 \quad (16)$$

Similar compounds were described in [37]: black monocrystals of composition $La_9Z_4I_{16}$ ($Z = N_{3.71}O_{0.29}$), $Ce_9Z_4I_{16}$ ($Z = N_{3.01}O_{0.99}$) and orange $BaLa_4Z_2I_8$ ($Z = N_{0.91}O_{0.09}$), $BaCe_4Z_2I_8$ ($Z = N_{1.96}O_{0.05}$) are formed as by-products in the synthesis of $BaLnI_4$.

An attempt of synthesizing cluster compounds of lanthanides with endohedral inclusions of transition metals gave compounds of composition $\{(C_2)_2O_2Dy_{12}\}I_{18}$ [38]. The reaction mixture consisting of Dy_{I3}, powdery dysprosium, iron and graphite is kept at 1000°C for 8 days in a pressurized tantalum container. A compound of a similar composition $\{(C_2)_2O_2Dy_{14}\}I_{24}$ [38] is obtained by the interaction of DyI_3, powdery dysprosium, dysprosium(III) oxide, graphite and sodium iodide used as a flux material. The synthesis is carried out also at 1000 °C for 10 days in a pressurized tantalum container. After slow cooling a flux with inclusions (black rectangular plates of the above composition) is obtained. All manipulations with the starting substances and products are carried out in an inert atmosphere. Compounds of composition $[M_9C_4O]I_8$ (M = Y, Ho, Er, Lu) are obtained similarly [39] (starting substances: MI_3, M_2O_3, M, C; temperature: 1050°C, tantalum container). When heating a mixture of Os, Lu and LuI_3 taken in a molar ratio of 2:4:5 in similar conditions (keeping at 1200 °C for 3 days with subsequent slow cooling within 13 days) black needle-shaped hydroscopic crystals of $[Os_5Lu_{20}]I_{24}$ [40] are obtained. Note that oxoiodide LuOI lutetium can be obtained in a similar way as a by-product of the interaction of powdery lutetium, rhenium, and lutetium iodide LuI_3 in a tantalum container at 950°C.

Thermal stability of oxoiodides

Lanthanide oxoiodides of composition LnOI are solid hydroscopic substances unstable with respect to light and air oxygen. Their color is close to that of the corresponding anhydrous iodides [4, 5, 14, 17, 19]. However, only in work [24] it is noted that keeping crystals of pure praseodymium oxoiodide for one year showed its stability to moisture and air. The hygroscopicity remains when alloying with iodides of alkaline metals, which was established by a study of constitutional diagrams of LnOI–MI (M = Na, K, Rb, Cs) [25] (fig. 2–4).

The thermal stability of oxoiodides in the air decreases while the REE atomic number grows. The decomposition of lanthanide oxoiodides proceeds through intermediate phases [20], the composition of which corresponds to the general formula nLnOI. Ln_2O_3, and ends with the formation of oxides Ln_2O_3. The decomposition temperatures of lanthanide oxoiodides and areas of the existence of the intermediate phases are shown in Tabl. 1.

Table 1. Thermal stability of some lanthanide oxoiodides

LnOI	Decomposition start, °C	Intermediate phases					Decomposition end, °C
		I $7\ LnOI{\cdot}Ln_2O_3$	II $4\ LnOI{\cdot}Ln_2O_3$	III $2LnOI{\cdot}\ Ln_2O_3$	IV $LnOI{\cdot}Ln_2O_3$	V $LnOI{\cdot}2Ln_2O_3$	
LaOI	355 [20]	–	–	650-730 [20]	–	–	830 [20]
NdOI	340 [20]	460-515 [20]	–	630 [20]	720-805 [20]		875 [20]
SmOI	335 [20]	460-510 [20]	560-620 [20]	640-800 [20]	–	–	885[20]
GdOI	315 [20]	–	–	430-560 [20]			
	> 400 [22]	–	–		450-550 [22]	–	–
DyOI	280 [14]	–	–	–	–	440-610 [11]	940 [14]
HoOI	390-490 [17]	–	490-520 [17]	–	–	–	970 [17]

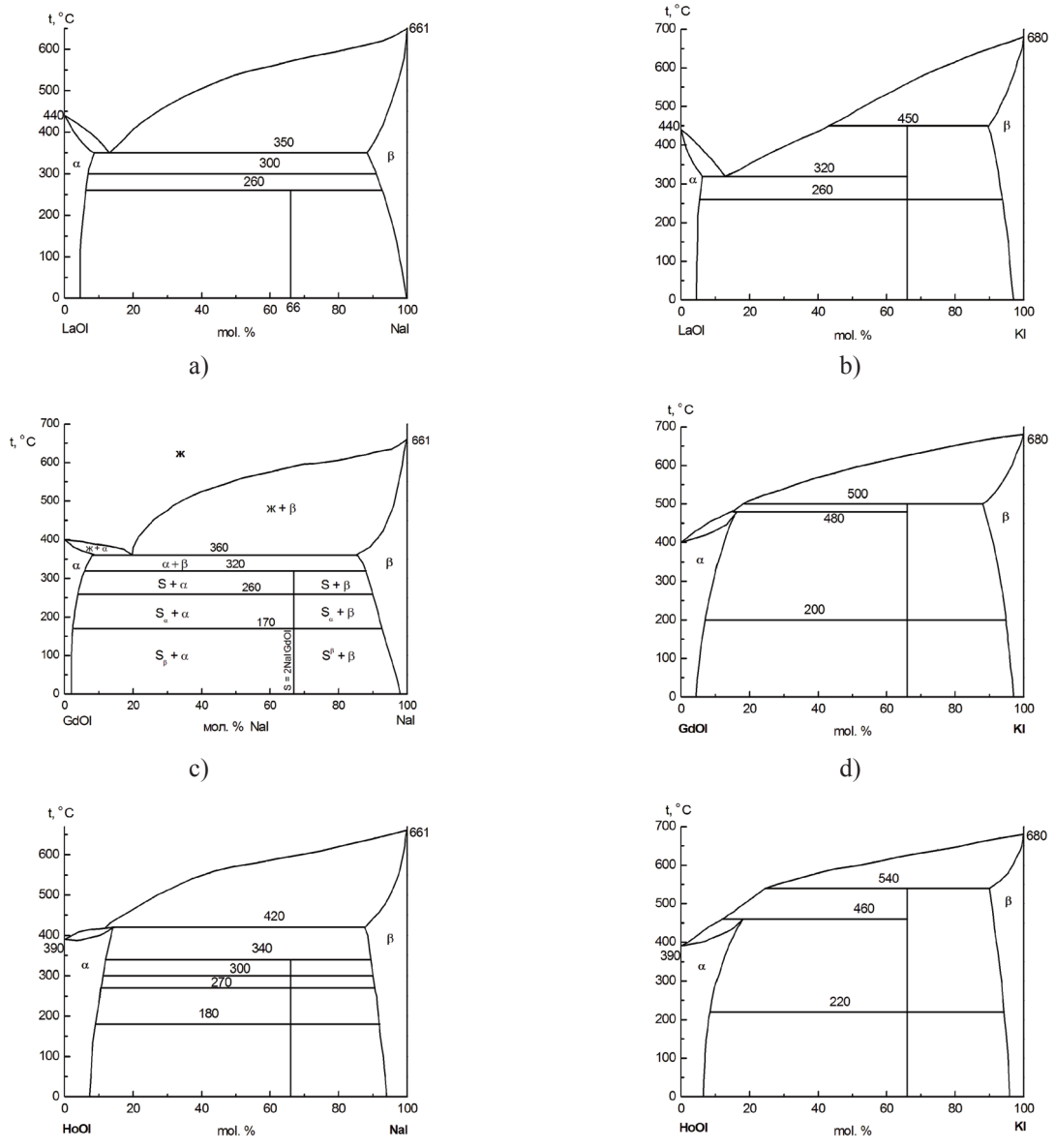

Fig. 2. Phase diagrams for systems: LaOI–MI (a–b), GdOI–MI (c, d), HoOI–MI (e, f). M = Na, K [17, 19].

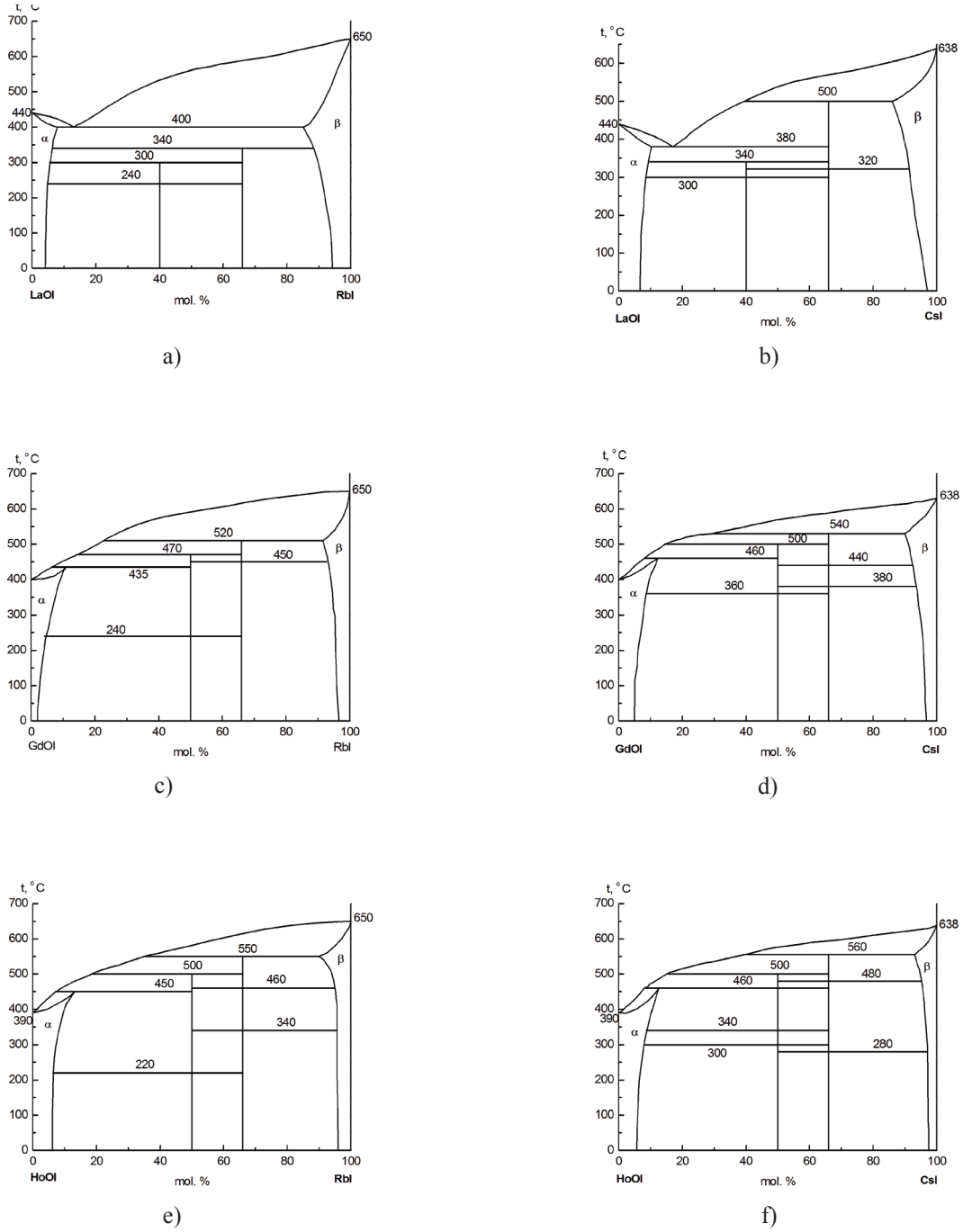

Fig. 3. Phase diagrams for systems: a) LaOI–RbI, b) LaOI–CsI, c) GdOI–RbI, d) GdOI– CsI, e) HoOI– RbI, f) HoOI– CsI [17, 19].

It can be seen from Table 1 that the thermal stability of the oxoiodides falls in the series from lanthanum to holmium: LaOI starts decomposing at 355°C, whereas NdOI, SmOI, GdOI – at 340, 335 and 315°C, respectively [20]. Unlike the temperatures of the decomposition start, the temperatures of the decomposition end tend to increase as the lanthanide atomic mass grows. Perhaps this is due to the formation of rather stable intermediate phases upon the decomposition of heavy lanthanide oxoiodides (Table 1).

REE oxoiodides are known [20] to decompose at lower temperatures than the corresponding oxobromides (300–450°C) and oxochlorides (500–800°C). The thermal stability of isostructural oxohalides considerably decreases along the series LnOCl–LnOBr–LnOI, which correlates with the layered structure of these compounds, because the interlayer distance increases from oxochlorides to oxoiodides.

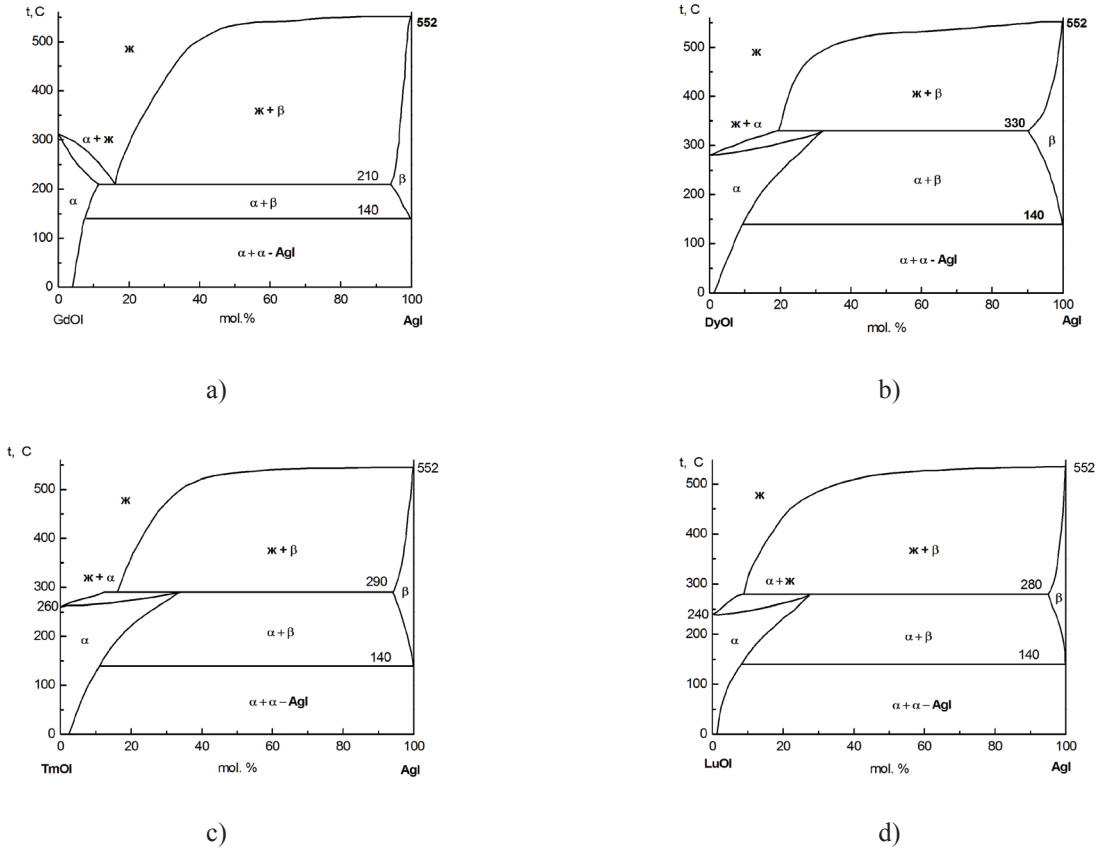

Fig. 4. Phase diagrams for systems: a) GdOI–AgI, b) DyOI–AgI, c) TmOI–AgI, d) LuOI–AgI [16].

Interaction of lanthanide oxoiodides with iodides of alkaline metals and silver iodide

In order to search new compounds based on lanthanide oxoiodides the phase diagrams of LnOI – MI (M = Na, K, Rb, Cs) were studied (Fig. 2, 3) [17, 19]. All the considered systems are of the eutectic type and are characterized by the formation of solid solutions based on both the lanthanide oxoiodide and the alkali metal iodide (types IV and V type of systems according to Roozeboom). For all the systems the formation of incongruently melting compounds of structure of LnOI:MI = 1:2 is typical. In LaOI–MI systems (M = Rb, Cs) in the solid phase at temperatures below the eutectic one compounds of composition LnOI:MI = 3:2 are formed, whereas in LnOI-MI systems (Ln = Gd, Ho, M = Rb, Cs) incongruently melting compounds of structure of LnOI:MI = by 1:1 are formed (Fig. 3). A crystallooptical study of the compounds showed [17] that all substances of composition MI·LnOI = 2:1, 1:1, 2:3 (Ln = La, Gd, Ho; M = Na, K, Rb, Cs) are optically anisotropic with the exception of optically isotropic crystals of MI·GdOI, RbI·HoOI and CsI·HoOI. The crystals of all the compounds have refraction indexes n > 1.63 [17].

In systems with the participation of silver iodide (types IV, V of systems according to Roozeboom, Fig. 4 [16]) no formation of ternary compounds is observed.

It can be seen from Fig. 2 and 3 that the presence of rather wide areas of solid solutions (from 3 to 7 mol %) indicates that iodides of alkali metals can efficiently embed in the crystal structure of a lanthanide oxoiodide, the specified area being capable of extending up to 25 mol % with growing temperature. Most likely, the formation of a solid solution of composition $Ln_{(1-x)}M_{(x)}O_{(1-x)}Vo_{(x)}I$ with oxygen vacancies Vo in the anion sublattice occurs. This is capable of exercising a significant influence on the increase in the mobility of cations and anions and on the growth of ionic conductivity. Most likely, the latter has anisotropic character due to the layered structure of oxoiodides. Besides, structural irregularities only in the oxygen sublattice of oxoiodides can lead to distortion of the flat structure of the oxygen layer and to decrease in the coherence of cationic tetrahedrons consisting of REE atoms. It should be noted that these effects are most obvious in systems with the participation of silver iodide, because the widest areas of solid solutions are found in these systems (Fig. 4).

Peculiarities of the structure of oxoiodides

According to [17], REE oxohalides are compounds with mixed anions, and their structure and properties

differ markedly from those of the corresponding Ln_2O_3 and LnI_3. Oxoiodides LnOI crystallize mainly in the structural type PbFCl (tetragonal crystal system, sp.gr P4/nmm) (Tab. 2, 3). In the structure of oxoiodides it is possible to distinguish parallel layers located in the following order: O–Ln–I–I–Ln–O. The distances of Ln–O and Ln–I do not undergo essential changes and remain almost constant for all oxohalides. On the contrary, the Ln–X' bond (X' is the iodide ion of the next layer) in the next layer is much longer than Ln–X, and this difference increases with decreasing ionic radius of Ln^{3+} ion. This leads to the formation of layered structures, in which each lanthanide cation is surrounded with four oxygen atoms and four iodide ions. The coordination polyhedron is a square antiprism, one of the quadrangular faces of which is formed by iodide ions, and the other one, by oxygen atoms. The antiprisms border the oxygen layer on both sides linking with each other through the common oxygen edges and triangular IOI sides. The double layers of the antiprisms are divided by layers of empty tetragonal pyramids of iodide ions [19]. According to [26], two-dimensional layers can be distinguished in the structure of LaOI. They are constructed of La_4O tetrahedrons with common edges and separated from each other by double layers of iodide ions. On the other hand, the structure of LnOI can be also presented in the form of layers of complex cations (LnO)+ alternating with the layers of iodide ions [17], Ln–I bonds being different. For example, in case of LuOI the average Lu–O bond length is 2.2 Å, and Lu–I distances are 3.314 and 4.015 Å. (In the second case the iodide ion belongs to the adjacent layer) (Fig. 5) [25, 41].

It is obvious from Table 2 that the volume of a unit cell monotonously increases with growing ionic radius, whereas the parameters of the tetragonal cells change as follows: parameter a linearly increases with increasing ionic radius (a = 2.17+1.51r, r is ionic radius [39]), and parameter c almost does not change. Therefore, the interlayer distances I–I–O practically do not change, whereas the cation "moves apart" the anions in the layer while its size increases.

The small interval of changes in parameter a of the unit cells along the series LaOCl–LaOBr–LaOI (4.11–4.14 Å) as compared to the significant increase in parameter c (the direction perpendicular to the planes of the layers) from 6.87 to 9.13 Å indicates considerable rigidity of the M_2O_2 system consisting of two layers of M atoms on both sides of the layer of oxygen atoms. Such type of tetragonal M–O–M layers is characteristic in particular of complex compounds of oxohalides [43]. At the same time in case of tetragonal oxohalides it is possible to find out the following regularity: while the sizes of the ions grow, parameter a increases, and parameter c decreases. Oxochlorides show the smallest change in parameter *a* and the greatest change in parameter *c*, whereas in case of oxoiodides the change in parameter *a* is more pronounced, and parameter *c* increases only by 0.063 Å upon transition from LaOI to LuOI.

As for scandium oxoiodide ScOI [25], it crystallizes in the structural FeOCl type. The coordination number of scandium is 7: there are 4 oxygen atoms and 3 iodine atoms in the vertices of the coordination polyhedron. Coordination number 7 is intermediate between 6 characteristic of ScOBr crystallizing in the structural FeOCl type and 8 as in case of LuOI [41] (Fig. 5). The Sc–I bond lengths change within a range of 2.89–3.26 Å, and the Sc–I bond lengths of Sc–O, within a range of 2.08–2.12 Å. The distance from the Sc atom to the next adjacent layer formed by iodide ions is 3.80 Å.

Tetrasamarium hexaiodide oxide $Sm^{II}_4OI_6$, similarly to many oxohalides of metals in the oxidation state +II of composition M_4OX_6, crystallizes in the structural type of anti-K_6HgS_4/ Na_6ZnO_4 with K_6HgS_4~I_6OSm_4 (hexagonal crystal system, sp.gr $P6_3mc$) [28]. An oxygen atom is located in the center of the tetrahedron formed by samarium atoms, and the tetrahedron itself is surrounded with 18 iodide ions, which take part in the formation of a three-dimensional, non-centrosymmetric arrangement. It should be noted that three iodide ions are μ_3-bridge ones, and they are located over the tetrahedron face, whereas six μ_2-bridge iodide ions are located over its edges, and the other nine I–ions are terminal ones [31, 35] (Fig. 6). Tetraeuropium hexaiodide oxide has a similar structure [32]. The Sm^{II}–Sm^{II} interatomic distances are equal to 3.9068(18) and 4.0133(14) Å, whereas they are slightly smaller in case of a similar europium compound: 3.8900(16) and 3.9796(14) Å. This is the consequence of lanthanide compression. It is interesting that the Ln–Ln interatomic distances in the considered oxoiodides are slightly shorter than in the corresponding metals (for example, the Eu–Eu interatomic distance in metallic europium is 3.99 Å). This indicates the formation of a weak Ln–Ln bond due to residual electron density [32]. A specific feature of the arrangement of these compounds is the presence of hexagonal channels extended along c axis in the structure. The diameter of a channel is about 4.86 Å (Fig. 6c). The phenomenon of lanthanide compression is seen as well in the lengths of the shortest Ln–O bonds: 2.39 (2), 2.436(7) Å (Ln = Sm) and 2.391(15), 2.416(5) Å (Ln = Eu) [31, 35].

In the $Eu^{II}_2OI_2$ structure [35] it is possible to distinguish also a little distorted Eu_4O tetrahedrons bound to each other in chains by means of the common edges located in trans position (Fig. 7a). The chains are surrounded with iodide ions, which, in turn, combine them in layers. On the contrary, the $Sm^{II}Sm^{III}O_2I$ crystal structure [33] is characterized by the formation of

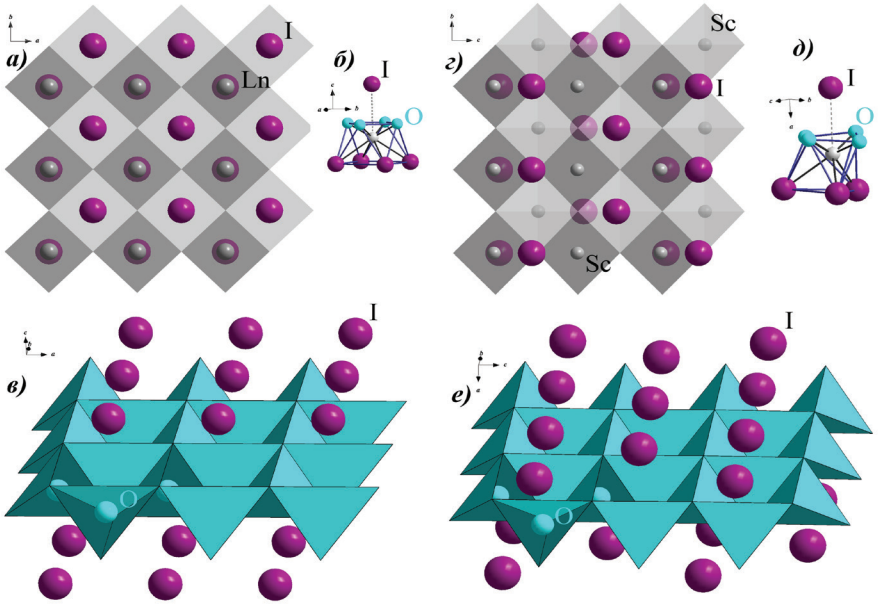

Fig. 5. Structure of REE oxoiodides [25, 41]: LnOI structure (a, b, c); ScOI structure (d, e, f);
a), d): view along the 4th order axis to the plane formed by the oxygen atoms;
b), e): corresponding coordination polyhedrons;
c), f) layers of the tetrahedrons constructed of the REE atoms around the oxygen atoms;
above and below: the layers of the iodine atoms.

Table 2. Crystallographic characteristics of lantanide oxoiodides

Compound	Sp.gr, Z	*a*, Å	*c*, Å	β°	V, Å^3	$P_{calc.}$ ($\rho_{exp.}$)
ScOI*[25]	C2/m, 8	19.333(6)	7.224(2)	93.51(3)	538.22	4.64
YOI [17]	P4/nmm 2	3.92	9.31	–	143.06	5.38
YOI [24]	P4/nmm 2	3.93	9.20	–	142.09	5.42
LaOI [19, 24, 26]	P4/nmm 2	4.144	9.126	–	156.72	5.97
LaOI [19]	P4/nmm 2	4.152	9.145	–	157.65	5.94
CeOI [19]	P4/nmm 2	4.098	9.157	–	153.78	6.11
PrOI [19, 24]	P4/nmm 2	4.086(2)	9.162(2)	–	152.96	6.16 (5.89 exp. [24] 6.19 calc. [17, 24])
NdOI [19]	P4/nmm 2	4.051	9.172	–	150.52	6.34
PmOI [19]	P4/nmm 2	4.010	9.180	–	147.62	6.48
SmOI [19, 24, 30]	P4/nmm 2	4.008(5)	9.192(8)	–	147.66	6.60 (6.59 [17]
EuOI [19, 24]	P4/nmm 2	3.993(1)	9.186(2)	–	146.46	6.69 (6.66 [17])
GdOI [19]	P4/nmm 2	3.968	9.191	–	144.71	6.89
TbOI [19]	P4/nmm 2	3.948	9.181	–	143.102	7.00
DyOI [14,19]	P4/nmm 2	3.936 3.935	9.183 9.180	–	142.26 142.15	7.13 (7.129 [17]) 7.14
HoOI [19]	P4/nmm 2	3.915	9.186	–	140.80	7.26
ErOI [19]	P4/nmm 2	3.902	9.172	–	139.65	7.38
TmOI [19, 24, 30]	P4/nmm 2	3.887(1)	9.166(2)	–	138.49	7.48
YbOI [19, 24, 30]	P4/nmm 2	3.870(6)	9.161(8)	–	137.20	7.65
LuOI [19]	P4/nmm 2	3.850	9.179	–	136.06	7.76
LuOI [25, 41]	P4/nmm 2	3.8585(7)	9.189(2)	–	136.81	7.717 [41]

* b = 3.8610(8)

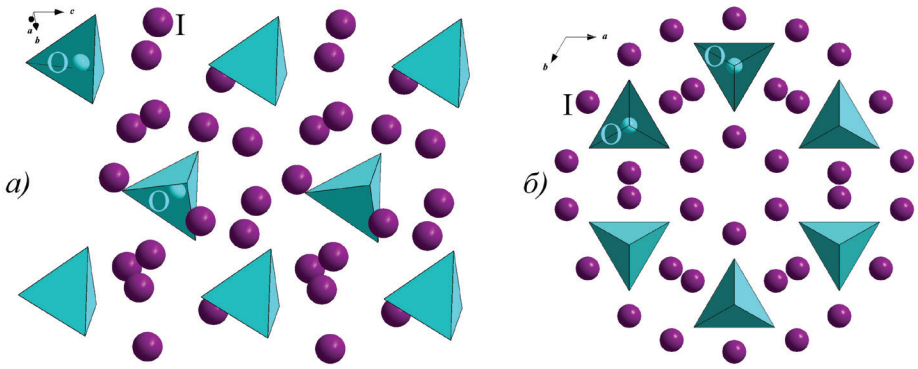

Fig. 6. Structure of Sm_4OI_6: a) tetrahedrons of Sm_4O surrounded with iodide ions of different types; b) fragment of $Sm^{II}_4OI_6$ structure (view along axis *c*) [31].

Table 3. Crystallographic characteristics of combined lanthanide oxoiodides

Compound	Syngony Sp.gr., Z	*a*, Å	*b*, Å	*c*, Å	Angle, °	V, Å^3	ρ_{calc}
Sm_2O_2I [17, 33]	Monocl. *C2/m*, 4	12.639(2)	4.100(1)	9.762(3)	β = 117.97(2)	446.8(2)	6.833
Sm_4OI_6 [13, 31]	Hex. $P6_3mc$, 2	10.4415(8)	–	8.0464(7)	–	759.73	6.027
Eu_2OI_2 [35]	Rhomb. *Imcb*, 4	6.489(1)	7.429(1)	13.071(3)	–	630.1	6.048
Eu_4OI_6 [32]	Hex. $P6_3mc$, 2	10.404(2)	–	7.996(3)	–	749.5	6.138
$La_9O_4I_{16}$ [36, 43]	Rhomb. *Fddd*	22.893(3)	43.156(6)	8.988(1)	–	8879.88	–
$La_9N_{3.71}O_{0.29}I_{16}$ [37]	Rhomb. *Fddd*, 8	22.893(3)	43.156(6)	8.988(1)	–	8880(2)	4.992
$Ce_9N_{3.01}O_{0.99}I_{16}$ [37]	Rhomb. *Fddd*, 8	8.900(1)	22.641(2)	42.795(4)	–	8623.0(2)	5.160
$BaLa_4N_{1.07}O_{0.93}I_8$ [37]	Monocl. *C2/c*, 4	8.975(1)	21.624(3)	12.293(2)	110.32(1)	2237.3(5)	5.160
$BaCe_4N_{1.96}O_{0.05}I_8$ [37]	Monocl. *C2/c*, 4	8.902(1)	21.497(3)	12.151(1)	110.25(1)	2181.5(5)	5.301
$\{(C_2)_2O_2Dy_{12}\}I_{18}$ [38]	Hex. *P6/m*, 8	20.2418(8)		12.9921(4)		4610.1(3)	6.158
$\{(C_2)_2O_2Dy_{14}\}I_{24}$ [38]	Tricl. P–1 1	9.7297(14)	10.3303(13)	16.770(2)	α = 101.424(11) β = 92.724(11) γ = 112.745(10)	1509.3(3)	5.942
$[Y_9(C_2)_2O]I_8$ [39]	Rhomb. *Pmmn*, 2	29.127(6)	3.8417(4)	10.8029(9)	–	1208.81	
$[Ho_9(C_2)_2O]I_8$ [39]	Rhomb. *Pmmn*, 2	28.867(3)	3.8157(4)	10.748(2)	–	11.8387	
$[Er_9(C_2)_2O]I_8$ [39]	Rhomb. *Pmmn*, 2	28.818(2)	3.8037(3)	10.7381(8)	–	1177.06	
$[Lu_9(C_2)_2O]I_8$ [39]	Rhomb. *Pmmn*, 2	28.333(2)	3.7575(3)	10.6377(9)	–	1132.50	
$[Os_5Lu_{20}]I_{24}$ [40]	Tricl. P–1 1	11.7330(17)	12.4841(17)	14.119(2)	α = 99.145(11) β = 107.663(11) γ = 108.844(11)	1787.7(4)	

layers consisting of the corresponding tetrahedrons bound through the vertices and the common edges located in cis position relatively to each other. They are separated from each other by layers of iodide ions (Fig. 7b). The Sm^{II} (Sm2) atoms are located in the center of a two-capped trigonal prism constructed of oxygen atoms and iodine, whereas the Sm^{III} (Sm1) atoms are situated in the center of a one-capped trigonal prism. The Sm^{II}–O bond lengths are equal to 2.40(2)–2.435(2) Å, which is comparable to the length of the SmII–O bond in Sm_4OI_6 (2.39(2), 2.436(7) Å) [31]. The lengths of the Sm^{III}–O bonds are 2.26(2)–2.35(2) Å, which is comparable to the sum of the ionic radiuses of Sm^{III} (1.02 Å, the coordination number is 7) and O^{2-} (1.38 Å) [42].

The crystal structure of compounds $La_9N_{3.71}O_{0.29}I_{16}$, $BaLa_4N_{1.07}O_{0.93}I_8$, $Ce_9N_{3.01}O_{0.99}I_{16}$ and $BaCe_4N_{1.96}O_{0.05}I_8$ [37] is characterized by the presence of Ln_4-tetrahedrons, in the center of which oxygen or nitrogen atoms (Tab. 3) are located. The Ln–Ln distances are equal to 3.42 and 3.95 Å in $La_9N_{3.71}O_{0.29}I_{16}$ and $BaLa_4N_{1.07}O_{0.93}I_8$, respectively, whereas they are equal to 3.69 and 3.87 Å in analogous cerium compounds. The Ln–O(N) distances change within narrower limits: 2.39 Å in $La_9N_{3.71}O_{0.29}I_{16}$ and 2.38 Å in $BaLa_4N_{1.07}O_{0.93}I_8$. In case of $Ce_9N_{3.01}O_{0.99}I_{16}$ and $BaCe_4N_{1.96}O_{0.05}I_8$ they are equal to 2.34 and 2.36 Å, which correlates well with the values of the sums of crystal radiuses [42] of the REE atom (coordination number is 6) and oxygen atom (coordination number is 4): La–O = 2.41 Å and Ce–O = 2.39 Å.

The structure of Ln_9Z_4I (Ln = La, Ce) is characterized by the presence of chains of Ln_4Z tetrahedrons (Z = O, N) having common edges in trans position relative to each other. The chains, in turn, are combined (via the iodide ions) in layers parallel to the [010] plane and

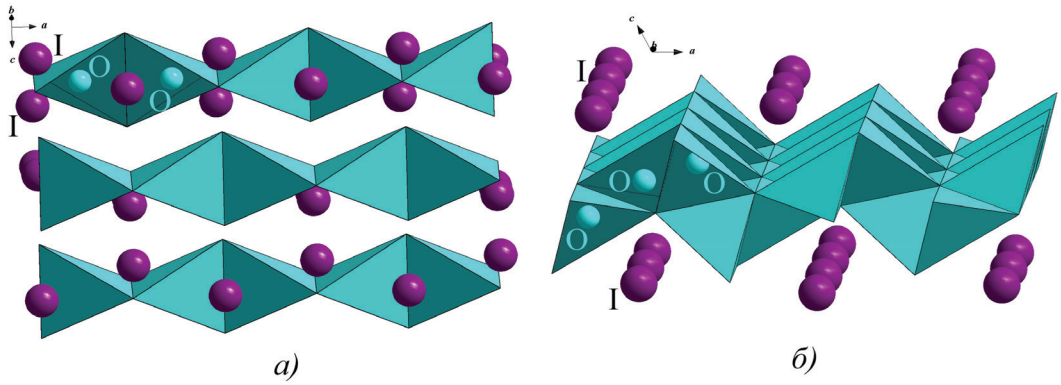

Fig. 7. Combinations of tetrahedrons constructed of REE atoms: a) chains of Eu_4O tetrahedrons bound with each other by means of common edges located in trans position (fragment of $Eu^{II}_2OI_2$ structure [35]); b) corrugated layers of Sm_4O tetrahedrons (fragment of $Sm^{II}Sm^{III}O_2I$ structure) [33].

Table 4. Structural characteristics of REE oxoiodides at various molar ratios Ln:O:I

Molar ratio Ln:O:I	General formula, oxidation degrees	Compound	Structure
1:1.5	M_2O_3 Ln^{+III}	Ln_2O_3	Three-dimensional framework
1:1.25:0.5	$M_4O_5I_2$ Ln^{+III}	Not found	Probably three-dimensional framework
1:1:0.5	M_2O_2I Ln^{+II} Ln^{+III}	Sm_2O_2I	Layered, corrugated layers
1:0.75:0.5	$M_4O_3I_2$ Ln^{+II}	Not found	Probably layered, corrugated layers
1:1:1	MOI Ln^{+III}	LnOI	Layered
1:0.5:1	M_2OI_2 Ln+II	Eu_2OI_2	Chain
1:0.75:1.5	$M_4O_3I_6$ Ln^{+III}	Not found	Probably chain
1:0.25:1.5	M_4OI_6 Ln^{+II}	Sm_4OI_6	Island
1:0.25:2.5	M_4OI_{10} Ln^{+III}	Not found	Probably island

turned by 45° relative to each other. Note the presence of a stacking force between these layers [36, 43]. The ninth atom of the lanthanide (according to formula $Ln[Ln_8Z_4]I_{16}$) is located in the center of the square anti-prism situated between these layers.

The structure of $BaLn_4Z_2I_8$ (Z = O, N) is interrelated with the structure of $Ln_9Z_4I_{16}$ compounds. The distinction is that $[BaI_8]$ polyhedrons are added. They are combined in chains turned with respect to the Ln_4Z chains. The Ba–I distances (3.60 Å) significantly exceed the La–I distances (3.46 Å) due to the different ion sizes. In general, the volume of the unit cell of compounds not containing barium exceeds that of $BaLn_4Z_2I_8$ approximately by four times [37].

In structures $\{(C_2)_2O_2Dy_{12}\}I_{18}$ and $\{(C_2)_2O_2Dy_{14}\}I_{24}$ [38] cluster tetramers can be found. They consist of a sequence of polyhedrons (octahedron–tetrahedron–tetrahedron–octahedron), in the vertices of which the dysprosium atoms are located, dumbbell-shaped fragments of two carbon atoms being situated in the center of the octahedrons, whereas the oxygen atoms are located in the centers of the tetrahedrons. In structure $\{(C_2)_2O_2Dy_{12}\}I_{18}$ chains of tetramers with common edges were found. Compound $\{(C_2)_2O_2Dy_{14}\}I_{24}$ is characterized by the presence of isolated tetramers (Fig. 8). The corresponding layers are located perpendicularly to c axis, and stacking force is implemented between them due to the Van der Waals forces. It is worth emphasizing that the dysprosium atoms are capable of forming clusters and chemical bonds with the endohedral atoms due to alternative electron configuration 4f95d1. (The Dy–Dy bonds lengths change within a range of 3.19–3.93 Å.) The Dy–O bond lengths in these compounds are equal to 2.1690(3)–2.2273(4) Å and are comparable to the Ln–O bond lengths in the Ln4O tetrahedrons: 2.39 (2), 2.436(7) Å (Ln = Sm) and 2.391(15), 2.416(5) Å (Ln = Eu) [31, 35]. Similar tetrahedral and octahedral clusters with common edges are typical also of $[M_9(C_2)_2O]I_8$ [36]. The role of endohedral atoms can be played not only by atoms of p-elements with rather high electronegativity, but also by atoms of transition elements, for example, osmium in $[Os_5Lu_{20}]I_{24}$ [40]. The $[Os_5Lu_{20}]I_{24}$ structure differs in that the chains are formed of four square anti-prisms and cubes having common square sides. The osmium atoms are located in these anti-prisms and cubes (Fig. 9a). The chains are surrounded with the iodide-ions (Fig. 9b), the Lu–I interatomic distances changing within a rather wide range [3.015 (3) –3.886 (3) Å] and are comparable to the Lu–I bond length in LuOI (3.314(1) Å) [25, 41]. The average values of the Lu–Lu bond lengths are 3.340–3.467 Å, and in case of Lu–Os, 2.819–2.933 Å, which exceeds the bond Lu–O lengths in LuOI (2.2048(5) Å) [25, 41]. The crystal arrangement of $[Os_5Lu_{20}]I_{24}$ corresponds to the closest hexagonal packing of $\{Os_5Lu_{20}\}$ chains due to the Van der Waals forces of [40] (Fig. 9c).

Note that the endohedral atoms are necessary to stabilize the REE clusters. The role of these atoms (or groups of atoms, for example, C_2) can be played by electronegative atoms of *p*-elements (oxygen, nitrogen, carbon, etc.) with coordination numbers equal to 4 and by atoms of transition elements with coordination numbers ≥ 6, the endohedral atoms (Z) in cluster complexes $\{ZnR_{4n}\}X_{(4n+4)}$ or $\{ZnR_{4n}\}X_{4n}$ being located in square anti-prisms or cube (coordination number is 8) [40, 44]. Clusters of this kind can be considered as complexes of anti-Werner type [40], in which the central atom is endohedral electronegative atom Z surrounded with electropositive atoms R forming the first coordination sphere, whereas the second coordination sphere is formed by electronegative atoms X (halide ions). This circumstance makes compounds of this kind similar to polioxometals of different structure, in which the coordination polyhedron of the endohedral lanthanide atom is frequently a square antiprism, in the vertices of which the oxygen atoms of $\{MO_6\}$ octahedrons are located (M = Mo, W) [46]. It is characteristic that the tendency of forming clusters remains in aqueous solutions as well. However, if there is an excess of water or OH– ions, larger octahedral $\{Ln_6O\}$ clusters, in which the REE atoms are bound with each other by μ_3-bridge OH groups, appear to be more stable [47–49]. Controlling the solution pH, the composition of the starting mixture of reagents (including even substances that are not included as a part of products), and controlling also the synthesis conditions makes it possible to obtain cluster compounds, in which the majority of fragments (or some of them) are bound with each other by means of hydrogen bonds or Van der Waals forces. They can be considered as precursors for forming of supramacrocompounds with unusual properties [50, 51].

Thus, in case of lanthanide oxoiodides of composition LnO_yI_z (per one mol of lanthanide) it is possible to deduce the following structural regularities: when the I:O molar ratio is 0–0.4, the compound is characterized by the presence of a three-dimensional framework. If this ratio changes within a range of 0.5–1, the structure is layered. When the I:O molar ratio is 2, the crystals are characterized by a chained structure that is transformed to an island structure at I:O = 6, 10 (Tab. 4). In the process, the length of the areas occupied with the iodide ions increases.

Let us consider compounds $La_9O_4I_{16}$, $\{(C_2)_2O_2Dy_{12}\}I_{18}$ and $\{(C_2)_2O_2Dy_{14}\}I_{24}$ (Tab. 4). In case of $La_9O_4I_{16}$ the Ln:O:I and I:O molar ratios are 1:0.444:1.778 and 4:1. According to the above criteria the structure of this

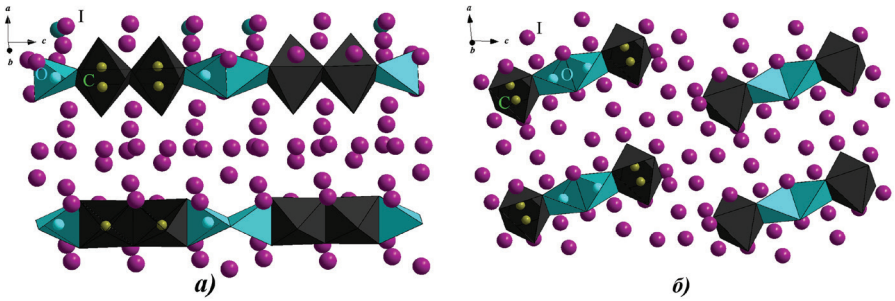

Fig. 8. Combinations of tetrahedrons Dy_4O and octahedrons $Dy_6(C_2)$:
a) chain (O-T-T-O-O-T-T-O)∞ of tetramers $\{(C_2)_2O_2Dy_{14}\}I_{32}$ with common edges in structure $\{(C_2)_2O_2Dy_{12}\}I_{18}$ [38];
b) tetramers $\{(C_2)_2O_2Dy_{14}\}I_{32}$ in structure $\{(C_2)_2O_2Dy_{14}\}I_{24}$ [38].

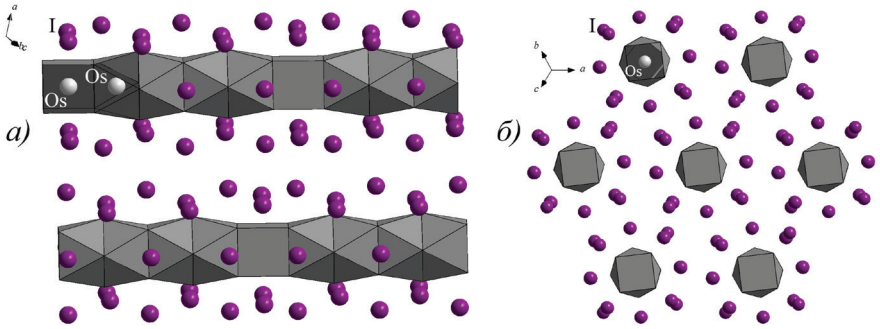

Fig. 9. Chains $\{Os_5Lu_{20}\}$ in $\{Os_5Lu_{20}\}$: a) cluster chains $\{Os_5Lu_{20}\}$ surrounded with μ_2- and μ_3-bridge iodine atoms;
b) relative positions of chains $\{Os_5Lu_2\}I_{24}$, projection to the plane (111) [40].

Table 5. Spectral data on luminescence excitation spectra and luminescence spectra of some REE oxoiodides

Element	Luminescence excitation	Luminescence	Compound	Literature
Pr	$^3H_4$–$^1D_2$ (605 nm)	$^1D_2$–$^3H_6$,$^3F_2$ (832–900 nm) $^1D_2$–$^3F_{3,4}$ (1015–1080 nm)	GdOI	[5]
Pr	$^3H_4$–$^1D_2$ (604 nm)	$^1D_2$–$^3H_6$,$^3F_2$ (830–895 nm) $^1D_2$–$^3F_{3,4}$ (1012–1078 nm)	LuOI	[5]
Nd	$^4I_{9/12}$–$^2G_{7/2}$ (584 nm); $^4I_{9/12}$–$^4G_{5/2}$ (597 nm)	$^4F_{3/2}$–$^4I_{9/2}$ (890–930 nm); $^4F_{3/2}$–$^4I_{11/2}$ (1070–1110 nm)	GdOI	[5] [22]
Nd	$^4I_{9/12}$–$^2G_{7/2}$ (583 nm); $^4I_{9/12}$–$^4G_{5/2}$ (597 nm);	$^4F_{3/2}$–$^4I_{9/2}$ (885-923 nm); $^2F_{5/2}$–$^2F_{7/2}$ (993-998 nm); $^4F_{3/2}$–$^4I_{11/2}$ (1070-1090 nm)	LuOI	[5]
Nd		$^4F_{3/2}$–$^4I_{9/2}$ (900-930 nm); $^4F_{3/2}$–$^4I_{11/2}$ (1080-1110 nm)	LaOI	[22]
Sm	$^6H_{5/2}$–$^4G_{5/2}$ (564 nm)	$^4G_{5/2}$–$^6H_{7/2}$ (601-617 nm); $^4G_{5/2}$–$^6H_{9/2}$ (647-660 nm); $^4G_{5/2}$–$^6H_{11/2}$ (705-722 nm)	GdOI	[5]
Sm	$^6H_{5/2}$–$^4G_{5/2}$ (565 nm)	$^4G_{5/2}$–$^6H_{5/2}$ (560 nm) $^4G_{5/2}$–$^6H_{7/2}$ (603-615 nm) $^4G_{5/2}$–$^6H_{9/2}$ (648-662 nm); $^4G_{5/2}$–$^6H_{11/2}$ (707-723 nm)	LuOI	[5]
Sm		$^4G_{7/2}$–$^6F_{3/2}$ (725 nm); $^4G_{5/2}$–$^6H_{11/2}$ (708 nm); $^4G_{7/2}$–$^6H_{13/2}$ (665 nm); $^4G_{5/2}$–$^6H_{9/2}$ (650 nm); $^4G_{7/2}$–$^6H_{11/2}$ (615 nm); $^4G_{5/2}$–$^6H_{7/2}$ (608 nm); $^4G_{7/2}$–$^6H_{9/2}$ (578 nm); $^4G_{5/2}$–$^6H_{5/2}$ (566 nm)	GdOI	[15]

compound has to be chain and intermediate between Eu_2OI_2 (chain) and Sm_4OI_6 (island) structures. When analyzing the structure of dysprosium compounds, it is necessary to consider that the framework contains octahedrons of dysprosium atoms around the couple of the carbon atoms (C_2). In this case it is possible to say that $(C_2)_2$ forming two octahedrons around themselves coordinate 12 dysprosium atoms that are equivalent to 3 tetrahedrons of dysprosium atoms around an oxygen atom. (The C_2 group in the structure can be considered to replace 1.5 oxygen atoms.) In case of $\{(C_2)2O_2Dy_{12}\}I_{18}$ the Ln:O:I and I:O molar ratios are 1:0.417:1.5 and 3.6, i.e., this compound, as well as $La_9O_4I_{16}$, belongs to the same range of molar ratios and is characterized by the presence of a chained framework (similar to Eu_2OI_2 structure). The structure of $\{(C_2)_2O_2Dy_{14}\}I_{24}$ is similar to the structure of Sm_4OI_6 and has an island framework (the Ln:O:I molar ratios are 1:0.357:1.714 and I:O = 4.8).

Luminescent properties

The excitation spectra and luminescence spectra of REE oxoiodides doped and not doped by activators were studied in works [4, 5, 15, 17, 23] (Tab. 5). Excitation consists in the transition of an electron to a higher energy level, and when the electron is subsequently transferred to a lower (main) level, energy is emitted, and light emission (luminescence) is observed. The search of perspective scintillation materials leads to the necessity of taking into account the density of a compound and its Zeff. The more these values, the better the material absorbs ionizing radiation [4] (Tab. 6, 7).

It is known [17] that the absorption bands of lanthanide ions can be classified as follows:

– in the far ultraviolet region (210–300 nm) the ions of some elements have absorption bands corresponding to allowed transitions 4f–5d (molar absorption coefficient ε = 300–700);

– broad intense absorption bands of lanthanide ions in the range of wavelengths 200–300 nm (ε = 400–750) due to charge transfer from O^{2-} to the activator ion in oxygen-containing crystal lattices;

– narrow 4f–4f absorption bands of lanthanides, the intensity of which in case of aqua ions is small (ε = 0.5–10).

The luminescence of Ho^{3+} ions is concentrated mostly in the infrared spectral range, that of Gd^{3+}, in ultraviolet, and those of other ions, in the visible and infrared spectral ranges. Depending on the composition the main spectral lines can be displaced and split into separate components [17].

It is important to note the promising outlook of using cerium-doped lanthanum oxohalides for obtaining new scintillation materials (Tab. 6) [23]. It can be seen from Tab. 6 that luminescence intensity increases

Table 6. Some properties of doped and undoped lanthanum oxohalides [23]

Compound	Syngony	Density, g/cm^3	Color	Luminance with respect to BGO	Radiation wavelength, nm
LaOBr	Tetragonal	6.13	White	0.3	370, 426
LaOBr : Ce (1%)	Tetragonal	6.13	White	0.9	422
LaOCl	Tetragonal	5.453	White	0.3	362
LaOCl : Ce (1%)	Tetragonal	5.453	White	0.5	412
LaOI	Tetragonal	5.914	Beige	0.05	380 408
LaOI : Ce (1%)	Tetragonal	5.914	Yellowish	0.3	370 408
$Bi_4Ge_3O_{12}$ (BGO)	Cubic	7.13	White	1	480

Table 7. Some properties of undoped REE oxoiodides [4]

Compound	Dopant, mol. %	Density, g/cm^3	Z_{eff}	Emission, nm	Luminescence with respect to $LaBr_3$:5% Ce^{3+}	Average lifetime in excited state, ns (≥ 10% of light)
YOI	Ce^{3+}, 1%	5.42	48	430, 480	0.07	23±0 (85%)
LaOI	Ce^{3+}, 2%	5.91	54	470	0.11	24±0 (86%)
GdOI	Ce^{3+}, 2%	6.85	56	440, 470	0.10	23±0 (67%)
LuOI	Ce^{3+}, 1%	7.71	59	430, 480	0.01	23±0 (82%) 73±1 (10%)

in all the cases due to the introduction of cerium(III) cations, the greatest effect among the oxohalides being found in case of lanthanum oxobromide [23]. Similar phenomena are found in case of lanthanum and yttrium oxoiodides [4].

The data of Table 7 show that the maximum light yield equal to 11% and 10%, respectively, with respect to LaBr3:5% Ce, was found in case of LaOI:2% Ce and GdOI:2% Ce.

Thus, the search of new materials based on lanthanide oxoiodides having good scintillation properties and not being hydroscopic is very promising. Apparently, obtaining cluster oxoiodides of complex composition having the necessary spectral characteristics will allow solving this problem.

References:

1. Yarovoj A.A., Revzin G.E., Petrova L.M. // Neorgan. Mater. (Inorganic Materials). 1971. V. VII. P. 437–441.
2. Work D.E. // Lighting Res. & Technol. 1981. V. 13. P. 143–152.
3. Groen C.P. Dissertation. University of Amsterdam. Faculty of Science. The Netherlands, 2012. 178 p.
4. Eagleman Y.D., Bourett-Courchesne E., Derenzo S.E. // J. Lumin. 2011. V. 131. P. 669–675.
5. Tararov A.V., Dubauskas G.J., Dudareva A.G., Zolin V.F. // Zh. Neorgan. Khimii. (Russ. J. Inorg. Chem.). 1991. V. 36. № 5. P. 1141–1144.
6. Furuya Y., Yanagida T., Fujimoto Y., Yokota Y., Kamada K., Kawaguchi N., Ishizu S., Uchiyama K., Mori K., Kitano K., Nikl M., Yoshikawa A. // Nucl. Instrum. Meth. A. 2011. V. A 634. P. 59–63.
7. van Eijk C.W.E. // Phys. Med. Biol. 2002. V. 47. P. R85–R106.
8. Bessiere A., Dorenbos P., van Eijk C.W.E, Krämer K.W., Güdel H.U., de Mello Donega C., Meijerink A. // Nucl. Instrum. Meth. A. 2005. V. A 537. P. 22–26.
9. Collin J., Giuseppone N., Van de Weghe P. // Coord. Chem. Rev. 1998. V. 178-180. P. 117–144.
10. Jaber N., Assie M., Fiaud J.-C., Collin J. // Tetrahedron. 2004. V. 60. P. 3075–3083.
11. Jantsch G., Skalla N. // Z. Anorg. Allg. Chem. 1930. V. 193. P. 391–405.
12. Jantsch G.,. Skalla N., Grubitsoh H. // Z. Anorg. Allg. Chem. 1933. V. 212. P. 65–83.
13. Brown D. Halides of lanthanides and actinides name. M.: Atomisdat, 1972. P. 222–223. (in Russ.).
14. Tararov A.V., Dudareva A.G. // Zh. Neorgan. Khimii. (Russ. J. Inorg. Chem.). 1991. V. 36. № 1. P. 44–46.
15. Tararov A.V., Dudareva A.G., Golovkova S.I. // Zh. Neorgan. Khimii. (Russ. J. Inorg. Chem.). 1991. V. 36. № 7. P. 1658–1661.
16. Tararov A.V., Dudareva A.G., Tupoleva A.A. // Zh. Neorgan. Khimii. (Russ. J. Inorg. Chem.). 1991. V. 36. № 5. P. 526–528.
17. Dudareva A.G. Khimiya bromidnykh i iodidnykh soedinenij lantanoidov (The chemistry of bromine and iodide of lanthanide compounds: monograph). M: Izd-vo Un-ta druzhby narodov, 1991. 165 p.
18. Batsanov S.S., Kopaneva L.I., Dorogova G.V. // Zh. Neorgan. Khimii. (Russ. J. Inorg. Chem.). 1982. V. 27. P. 2150–2154.
19. Molodkin A.K., Tupoleva A.L., Dudareva A.G. // Zh. Neorgan. Khimii. (Russ. J. Inorg. Chem.). 1989. V. 34. № 5. P. 1295–1302.
20. Hölsä J.P.K. // J. Therm. Anal. 1982. V. 25. P. 127–133.
21. Hölsä J., Niinistö L. // Thermochim. Acta. 1980. V. 37. P. 155–160.
22. Molodkin A.K., Tupoleva A.L., Dudareva A.G., Zolin V.F., Ezhov A.I. // Zh. Neorgan. Khimii (Russ. J. Inorg. Chem.). 1988. V. 33. № 5. P. 1289–1293.
23. Porter-Chapman Y.D., Bourret-Courchesne E., Taylor S.E., Weber M.J., Derenzo S.E. Systematic Search for New Lanthanum Scintillators // IEEE Nuclear Science Symposium Conference Record. 2006. V. 3. P. 1578–1582.
24. Potapova O.G., Vasil'eva I.G., Borisov S.V. // Zh. Struct. Khimii. (Russ. J. Struct. Chem.). 1977. V. 18. № 3. P. 573–577.
25. Zimmermann S., Meyer G. // Z. Anorg. Allg. Chem. 2008. V. 634. P. 2217–2220.
26. Welberry T.R., Williams Z.B. // J. Appl. Crystallogr. 1985. V. 18. P. 362–364.
27. Brown D., Hall L., Hurtgen C., Moseley P.T. // J. Inorg. Nucl. Chem. 1977. V. 39. P. 1464–1466.
28. Brauer G. Rukovodstvo po neorganicheskomu sintezu: v 6 t. T. 4.: per. s nem. (A guide to inorganic synthesis: in 6 vol. V. 4:/ transl. from Germ.) / Ed. by G. Brauer. M.: Mir, 1985. P. 1175–1177. (in Russ.).
29. Shvetsova Z.N., Drobot D.V., Igumnova N.M. // Zh. Neorgan. Khimii (Russ. J. Inorg. Chem.). 1973. V. 18. № 9. P. 2555–2558.
30. Kruse F.H., Asprey L.B., Morosin B. // Acta Crystallogr. 1961. V. 14. P. 541–542.
31. Hammerich S., Pantenburg I., Meyer G. // Acta Crystallogr. E. 2005. V. E 61. P. i234–i236.
32. Liao W., Dronskowski R. // Acta Crystallogr. C. 2004. V. C60. P. i23-i24.
33. Ryazanov M., Hoch C., Mattausch H., Simon A. // Z. Anorg. Allg. Chem. 2006. V. 632. P. 2385–2388.

34. Antonenko T.A., Simonenko N.P., Albov D.V., Simonenko E.P., Alikberova L.Yu. Sposob polucheniya oksida-diiodida dievropiya Eu2OI2: pat. 2485050 Russian Federation. № 2012101943/05; appl. 20.01.2012; publ. 20.06.2013.

35. Hammerich S., Meyer G. // Z. Anorg. Allg. Chem. 2006. V. 632. P. 1244–1246.

36. Meyer G., Gerlitzki N., Hammerich S. // J. Alloy. Compd. 2004. V. 380. P. 71–78.

37. Gerlitzki N., Hammerich S., Pantenburg I., Meyer G. // Z. Anorg. Allg. Chem. 2006. V. 632. P. 2024–2030.

38. Daub K., Meyer G. // Z. Anorg. Allg. Chem. 2010. V. 636. P. 1716–1719.

39. Mattfeld H., Krämer K., Meyer G. // Z. Anorg. Allg. Chem. 1993. V. 619. P. 1384–1388.

40. Brühmann M., Mudring A.-V., Valldor M., Meyer G. // Eur. J. Inorg. Chem. 2011. P. 4083–4088.

41. Zimmermann S., Meyer G. // Acta Crystallogr. E. 2007. V. E63. P. i193.

42. Shannon R.D. // Acta Crystallogr. A. 1976. A32. P. 751–767.

43. Gerlitzki N., Meyer G. // Z. Anorg. Allg. Chem. 2002. V. 628. P. 2199.

44. Wells A.F. Strukturnaya neorganicheskaya khimiya (Structural Inorganic Chemistry). M.: Mir, 1987. V. 2. P. 181–185. (in Russ.).

45. Rustige C., Bruhmann M., Steinberg S., Meyer E., Daub K., Zimmermann S., Wolberg M., Mudring A.-V., Meyer G. // Z. Anorg. Allg. Chem. 2012. V. 638. P. 1–11.

46. Bassil B.S., Kortz U. // Z. Anorg. Allg. Chem. 2010. V. 636. P. 2222–2231.

47. Rukk N.S., Albov D.V., Skryabina A.Yu., Osipov R.A., Alikberova L.Yu. // Koord. Khimiya (Russ. J. Coord. Chem.) 2009. V. 35. № 1. P. 14–16.

48. Wang R., Carducci M.D., Zheng // Inorg. Chem. 2000. V. 39. 1836–1837.

49. Zhang D.-S., Ma B.-Q., Jin T.-Z., Gao S., Yan C.-H., Mak T.C.W. // New J. Chem. 2000. V. 24. P. 61–62.

50. Lehn J.M. Supramolecular Chemistry-Scope and Perspectives Molecules, Supermolecules, and Molecular Devices (Nobel Lecture) // Angew. Chem. Int. Ed. 1988. V. 27. P. 89–112.

51. Lehn J.M. Perspectives in Chemistry: from Supramolecular Chemistry towards Adaptive Chemistry // Plenary Lecture at the 4th EuCheMs chemistry congress, August 26–30, 2012. Prague, Czech Republic. S. 588.